

SUPPLEMENTARY TABLE

Supplementary Table 1. SAXS data collection and analysis statistics

mMLKL 1-169; C169S

Data-collection parameters	
Instrument	Australian Synchrotron SAXS/WAXS beamline
Beam geometry	120 micron point source
Wavelength (Å)	1.033
Exposure time	2 sec exposures
Temperature (K)	285
q range (Å ⁻¹) ^a	0.00912 to 0.400
Protein concentration	50 µL of 7 mg/ml protein <i>via</i> inline gel filtration chromatography 0.2M NaCl, 20mM HEPES pH 7.5
Structural parameters	
I(0) (cm ⁻¹) [from P(r)]	0.03664 ± 0.0002
R _g (Å) [from P(r)]	31.55 ± 0.14
D _{max} (Å)	100
I(0) (cm ⁻¹) (from Guinier)	0.03600 ± 0.0002
R _g (Å) (from Guinier)	31.30 ± 0.32
Software employed	
Primary data reduction	Scatterbrain (Australian Synchrotron)
Data processing	PRIMUS, GNOM
Computation of model intensities	CRYSOL
Rigid body fitting	SASREF

^a q is the magnitude of the scattering vector, which is related to the scattering angle (2θ) and the wavelength (λ) as follows: $q = (4\pi/\lambda)\sin\theta$

SUPPLEMENTARY FIGURE LEGENDS

Supplementary figure 1. SDS-PAGE of all mMLKL NTD purified constructs, CD spectroscopy, and supplementary AUC spectra. (a) Each purified protein construct was resolved by reducing SDS-PAGE to assess purity. (b) Circular dichroism spectroscopy showing mMLKL NTD constructs retain α -helical secondary structure. All constructs show double-minima at 208 nm and 222 nm respectively. Each point on the curve is a mean of 4 second averaging at each wavelength. (c-h) Sedimentation velocity analytical ultracentrifugation data. Raw radial absorbance data (circles) are shown overlaid with the best fit to the continuous sedimentation coefficient [c(s)] distribution model (solid lines). Radial absorbance scans collected at 18 minute intervals during sedimentation are shown.

Supplementary figure 2. Cellular activity of MLKL bearing second brace helix mutations parallels behaviour of recombinant proteins. Complete dataset, including uninduced vs dox-induced and TS only controls, for experiments presented in Figure 2. TNF (T); Smac-mimetic (S); emricasan (IDN-6556; I); Q-VD-OPh (Q). (a-d) Wild-type and *Mlkl*^{-/-} MDFs had full-length mMLKL harbouring the indicated alanine substitutions stably incorporated under the control of a doxycycline (dox) inducible promoter using lentiviral infection. Cells were either left untreated (UT), treated with TS (apoptosis) or treated with TSI or TSQ (necroptosis) 3 hrs post dox induction. Cell death was measured using PI staining and flow cytometry 24 hours after death stimulation. Cell death data are the mean \pm SEM of three independent experiments with 2-3 biologically independent replicates per experiment (n=6-9). The dox-induced (white bars), untreated (UT) and TSQ-stimulated data are shown in Figure 2.

Supplementary figure 3. Western blots showing inducible expression of alanine scanning mutagenesis MLKL constructs with addition of doxycycline. (a) *Mlkl*^{-/-} MDFs reconstituted with wild-type full length mMLKL. (b-e) Wild-type and *Mlkl*^{-/-} MDFs expressing full length MLKL with indicated alanine mutations. Each line has either two or three biological replicates (indicated by #1 and #2 for wild-type; #391, #392 and #393 for *Mlkl*^{-/-}). Actin was used as a loading control.

Supplementary figure 4. Chimeric mouse:human MLKL constructs reveal key determinants for constitutive killing of human and mouse cell lines. Complete dataset, including uninduced vs dox-induced and TS only controls, for experiments presented in Figure 4. (a, c, e, g, i) Wild-type, *Mlkl*^{-/-} and *Mlkl*^{-/-} *Ripk3*^{-/-} MDFs were stably transfected with doxycycline inducible chimeric constructs. In the presence or absence of dox, cells were either left untreated (UT) or stimulated with TS, or TSQ/TSI. Cell death was analysed by PI uptake 24 hours after death stimuli. Data are the mean \pm SEM of three independent experiments with 2-3 biologically independent replicates per experiment (n=6-9).

(b, d, f, h) Human cell lines, HT29 and U937, stably transduced with doxycycline inducible chimeric constructs. Cell death assays were performed similarly to MDFs, except that cell death was measured 48 hrs after death stimulus for human cell lines. Data are the mean \pm SEM of 3 independent experiments (n=3), except for (h) where n=2 for U937 cells. The dox-induced (white bars), untreated (UT) and TSQ-stimulated data are shown in Figure 4.

Supplementary figure 5. Western blots showing inducible expression of chimeric MLKL constructs with addition of doxycycline in MDFs, U937 and HT29 cells. (a) HT29 cells reconstituted chimeric MLKL (one biological replicate per chimera). (b) U937 cells reconstituted chimeric MLKL (one biological replicate per chimera). (c-g) Either wild-type and *Mlkl*^{-/-} MDFs, or wild-type and *Mlkl*^{-/-} and *Mlkl*^{-/-} *Ripk3*^{-/-} MDFs expressing chimeric

constructs. Each MDF line has either two or three biological replicates (indicated by #1, #2 and #3 for wild-type; #391, #392 and #393 for *Mlkl*^{-/-}; #24, #25 and #26 for *Mlkl*^{-/-} *Ripk3*^{-/-}). Actin was used as a loading control.

Supplementary figure 6. Residue swaps between human and mouse brace region suggest distinct roles for the first and second brace helix. Complete dataset, including uninduced vs dox-induced and TS only controls, for experiments presented in Figure 5.

(a-f) Wild-type and *Mlkl*^{-/-} MDFs were stably transfected with doxycycline inducible chimeric constructs harbouring the indicated mutations. Cells were stimulated with TS, TSQ or TSI and cell death was measured by PI uptake and flow cytometry. Death assays represent mean ± SEM of three independent experiments with 2-3 biologically independent replicates per experiment (n=6-9). The dox-induced (white bars), untreated (UT) and TSQ/TSI-stimulated data are shown in Figure 5.

Supplementary figure 7. Western blots showing inducible expression of residue swapped chimeric MLKL constructs with addition of doxycycline in MDFs. (a-f) Wild-type and *Mlkl*^{-/-} MDFs expressing residue swapped chimeric constructs. Each MDF line has either two or three biological replicates (indicated by #1, #2 and #3 for wild-type; #391, #392 and #393 for *Mlkl*^{-/-}). Actin was used as a loading control.

SUPPLEMENTARY METHODS

Circular dichroism spectroscopy

Circular dichroism (CD) spectroscopy experiments were performed on the Aviv Circular Dichroism Spectrometer, Model 430. Proteins between 0.15-0.5 mg/ml were analysed in TBS (150 mM NaCl, 20 mM Tris-HCl, pH 7.5) with 1mM TCEP. Sample was placed in a 0.1 cm pathlength quartz cuvette, and readings taken between 190–260 nm, with 4 second averaging at each wavelength. Buffer blank adjusted readings were converted from machine units (millidegrees) to mean residue ellipticity (MRE) by the following formulae:

$$MRE = \frac{Machine\ units \times MRW}{10 \times pathlength \times protein\ concentration} \quad (deg.cm^2.dmol^{-1}.residue^{-1})$$

Where MRW = Mean residue weight, pathlength is cm, concentration is mg/ml.

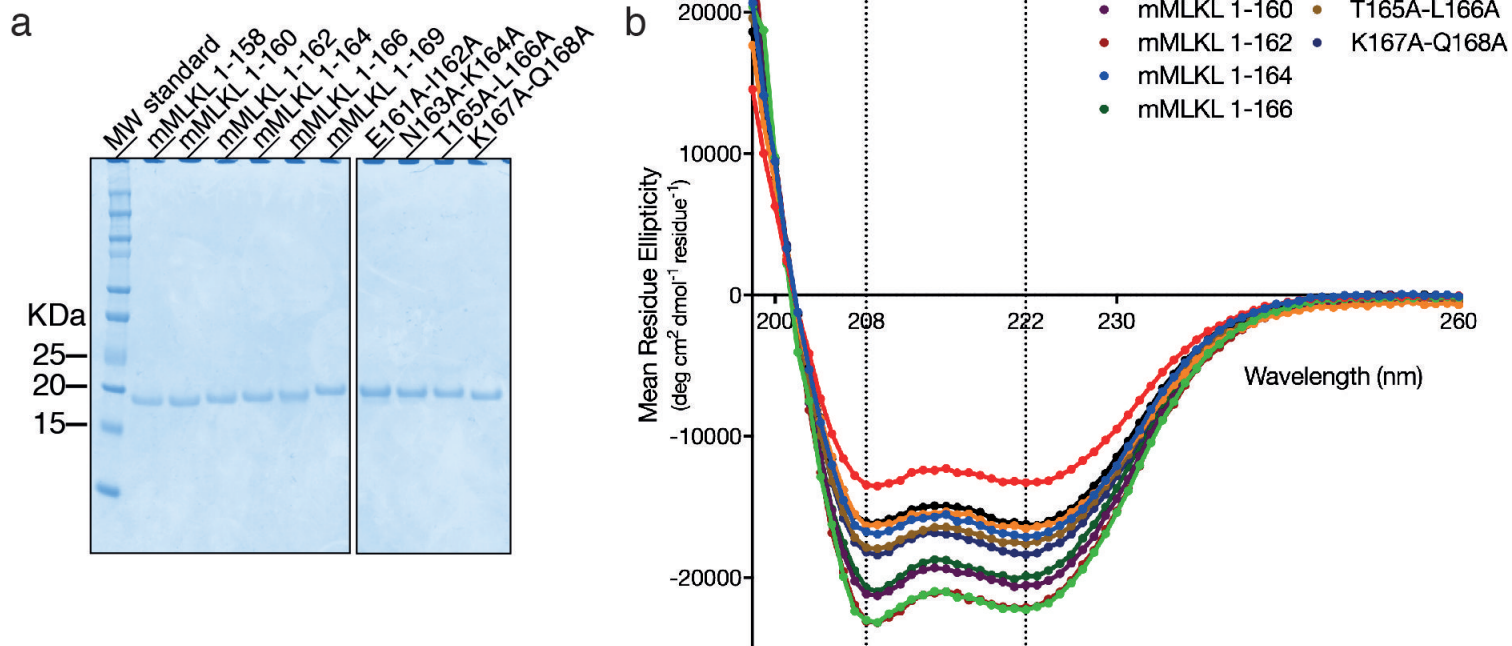
$$MRW = \frac{Molecular\ weight\ (Da)}{Number\ of\ residues} \quad (Da.residue^{-1})$$

(<http://dichroweb.cryst.bbk.ac.uk/html/home.shtml>¹)

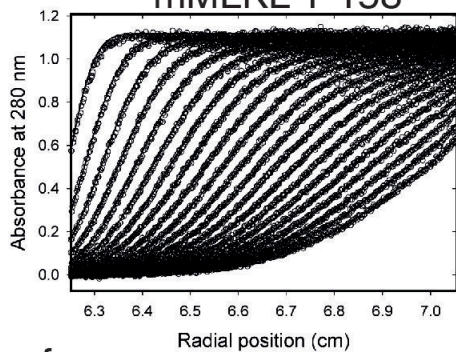
SUPPLEMENTARY REFERENCE

1. Lobley A, Whitmore L, Wallace BA. DICHROWEB: an interactive website for the analysis of protein secondary structure from circular dichroism spectra. *Bioinformatics* 2002, **18**(1): 211-212.

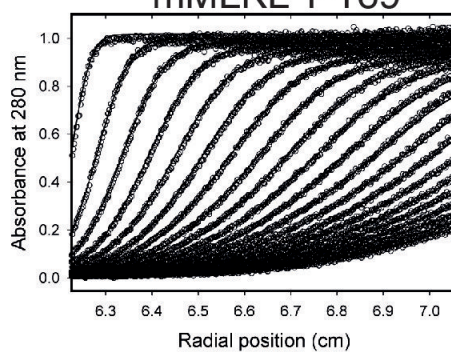
Supplementary figure 1



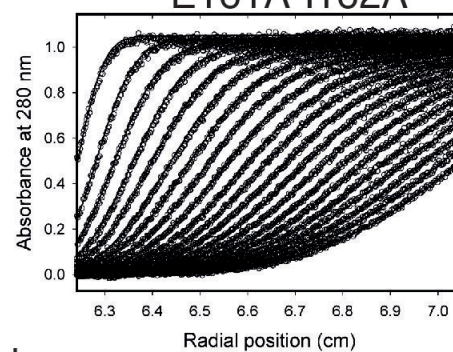
c mMLKL 1-158



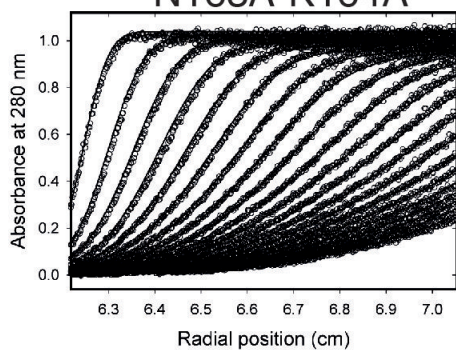
d mMLKL 1-169



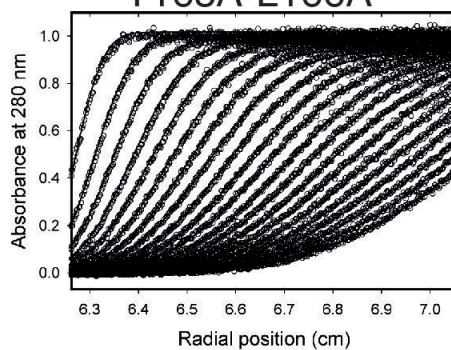
e E161A-I162A



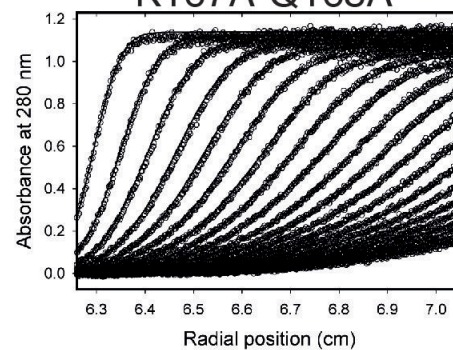
f N163A-K164A



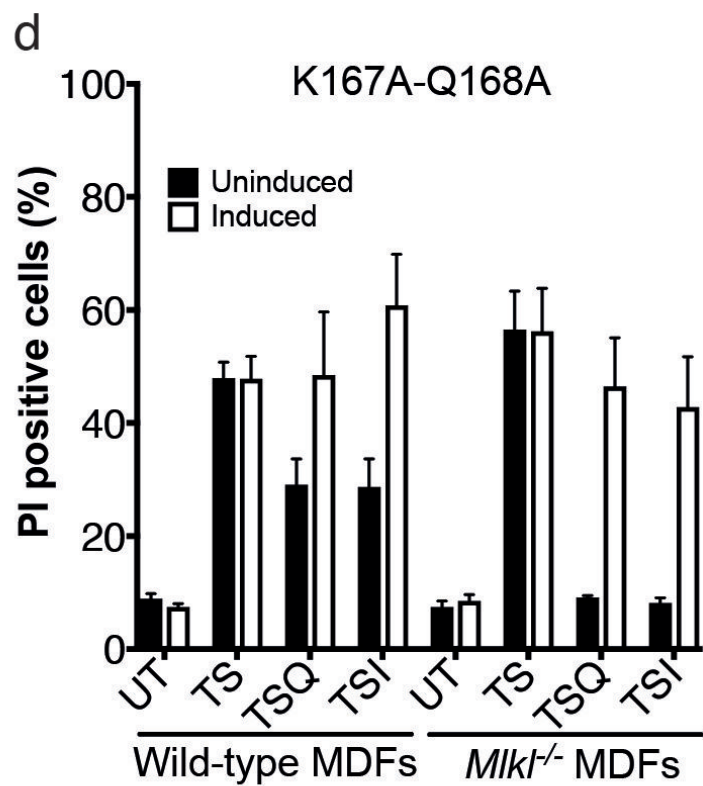
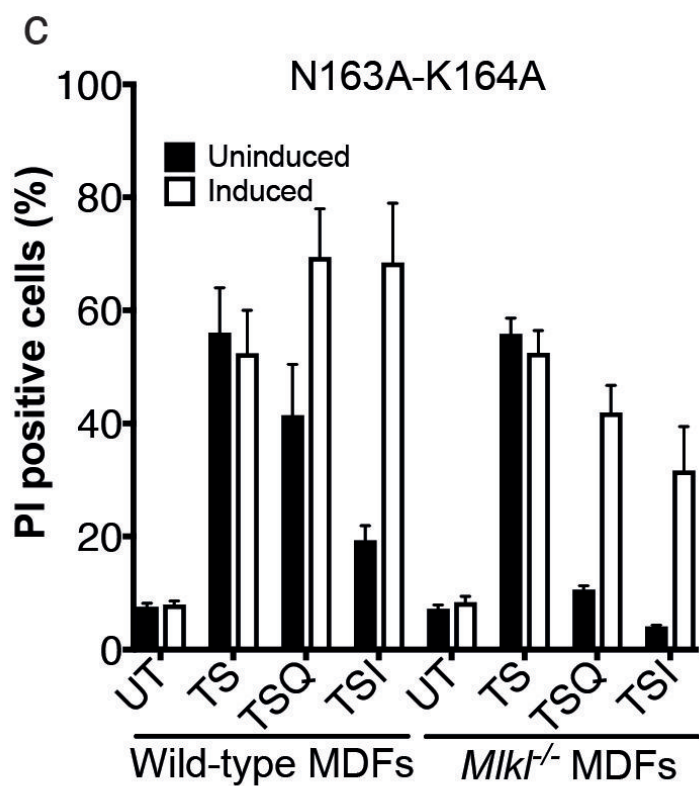
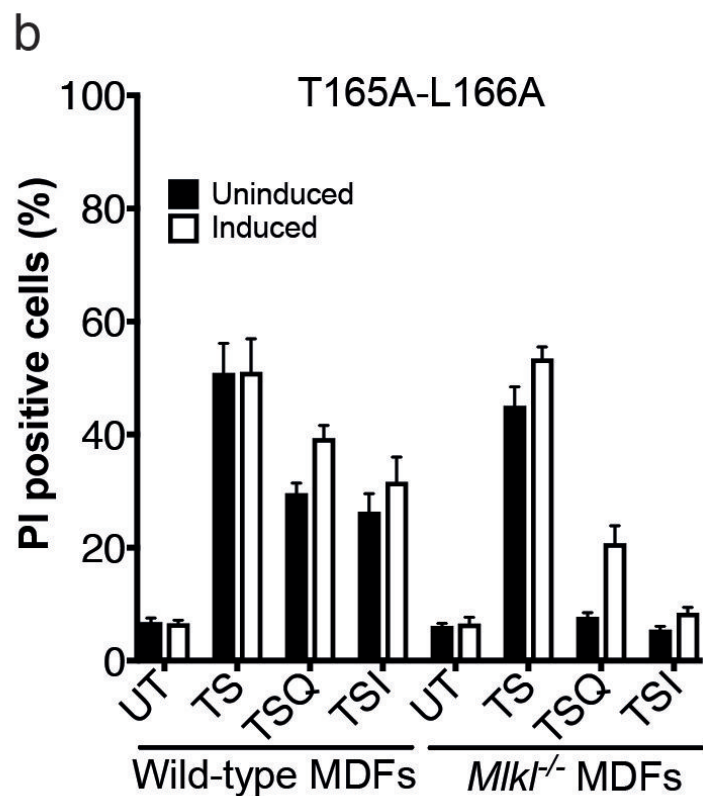
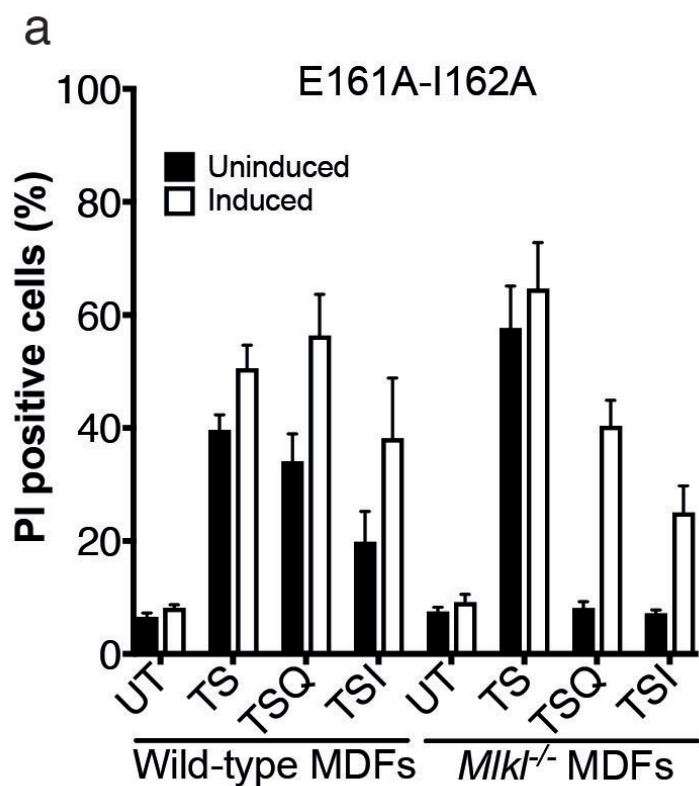
g T165A-L166A



h K167A-Q168A



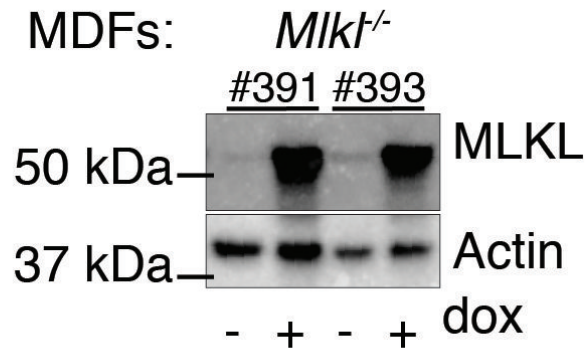
Supplementary figure 2



Supplementary figure 3

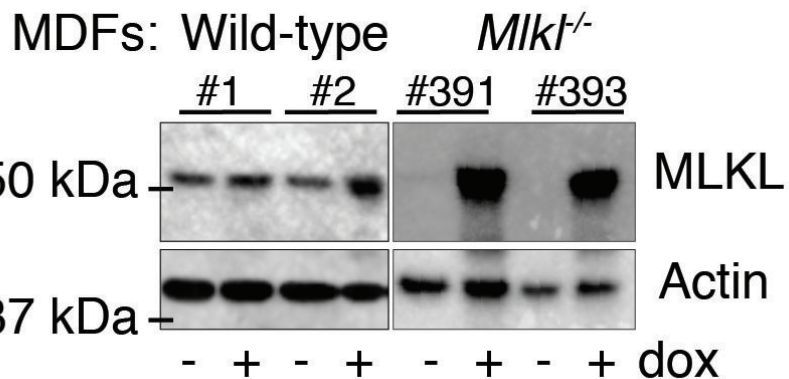
a

Wild-type mMLKL (1-464)



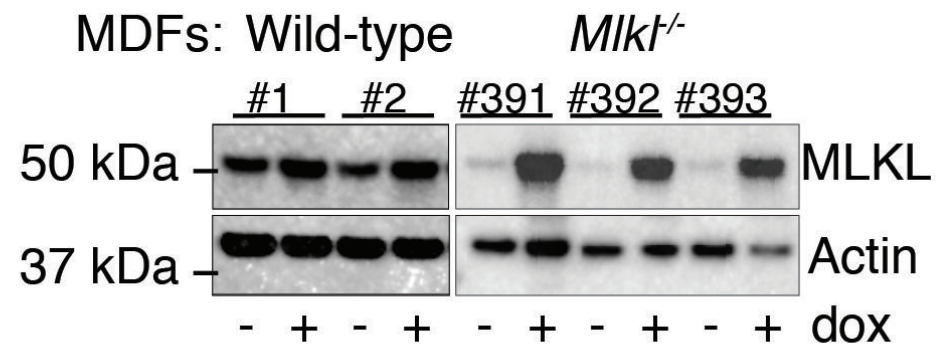
b

E161A-I162A



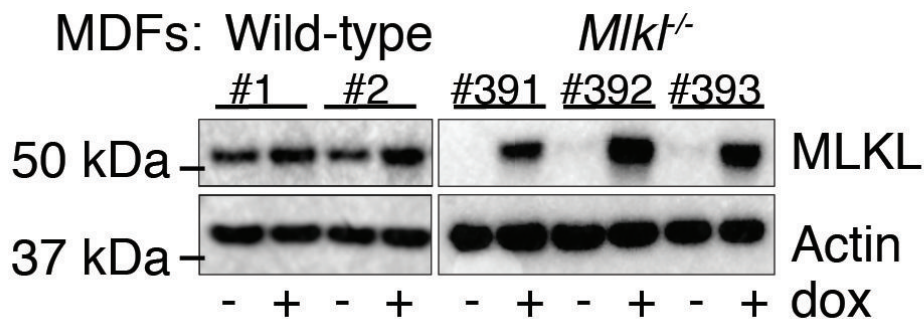
c

N163A-K164A



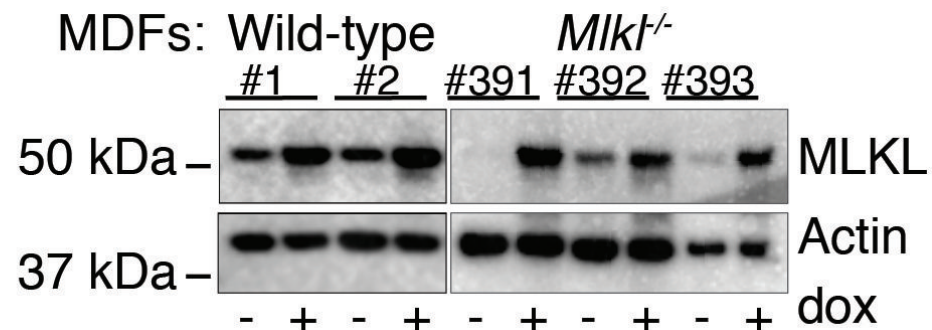
d

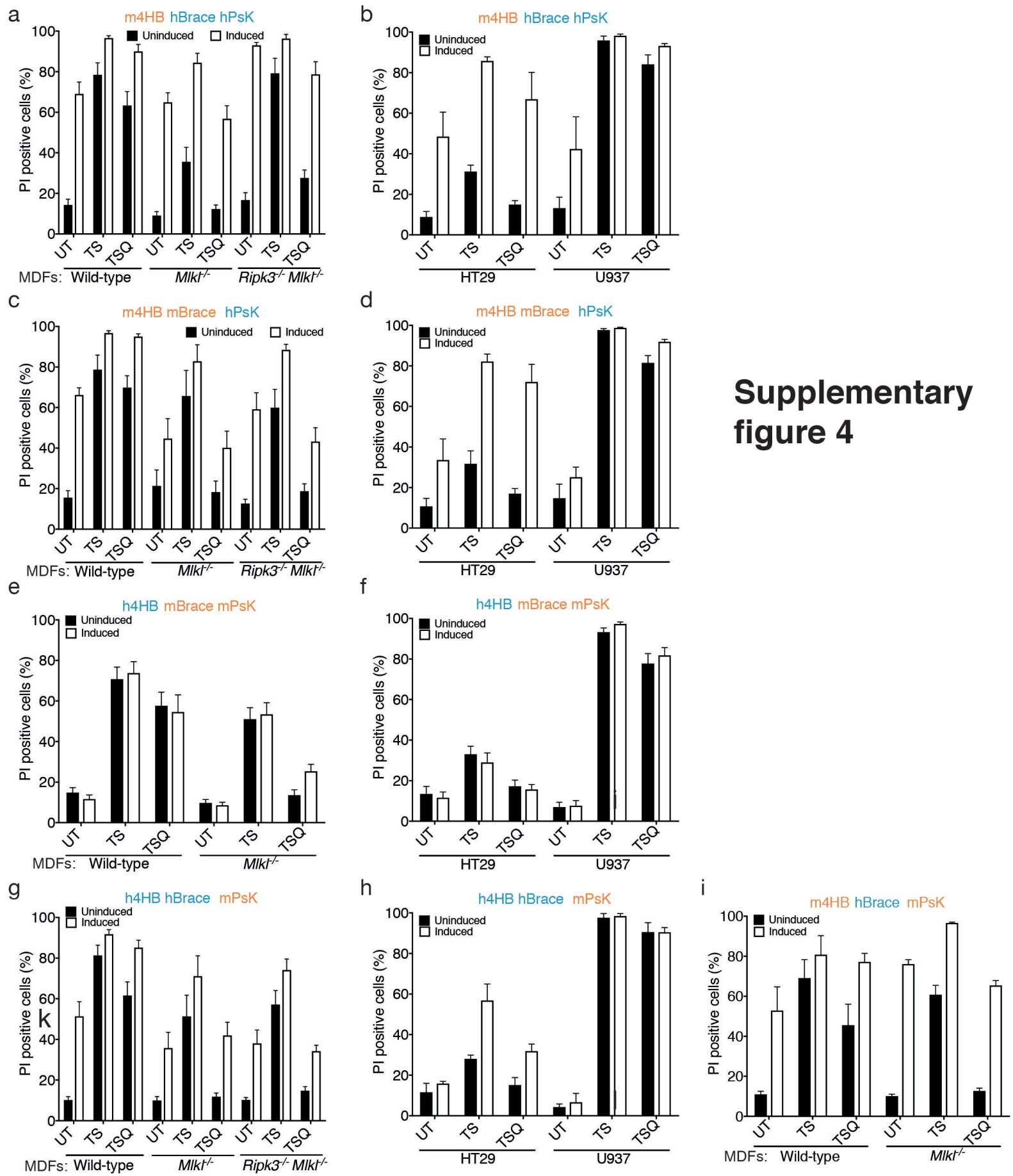
T165A-L166A



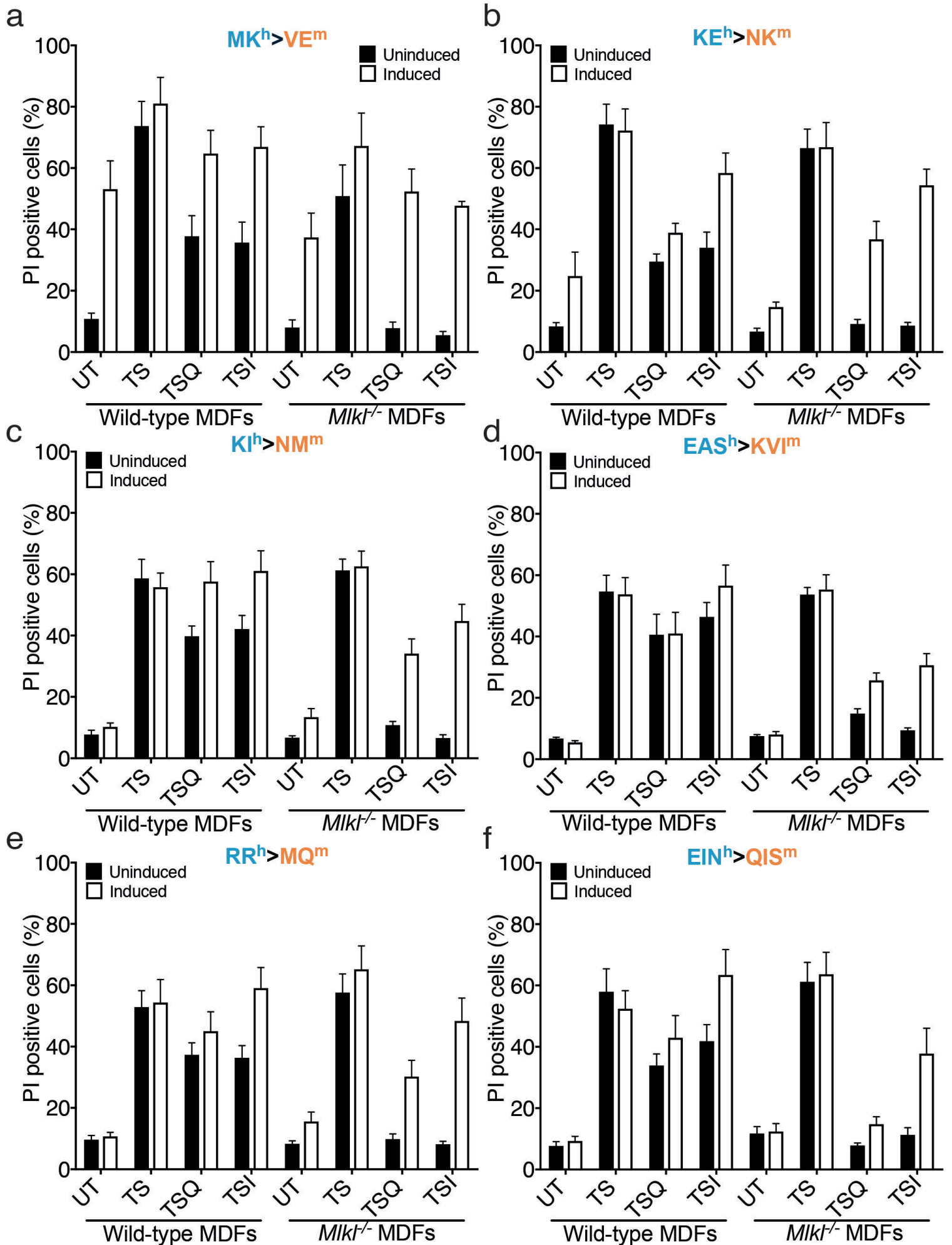
e

K167A-Q168A





Supplementary figure 6



Supplementary figure 7

